EUDET-Memo-2009-24

# CALICE Test Beam Data and Hadronic Shower Models

Riccardo Fabbri

on behalf of the CALICE Collaboration
FLC, DESY, Notkestrasse 85, 22607 Hamburg, Germany
E-mail: Riccardo.Fabbri@desy.de

January 14, 2010

**Abstract**

The CALICE collaboration has constructed a hadronic sandwich calorimeter prototype with 7608 scintillating plates, individually read out by multi-pixel silicon photomultipliers (SiPMs). For the first time ever the readout is performed using SiPMs on a large scale. Results of test beam operations with muon, positron and hadron beams at CERN are presented here, validating the feasibility of the novel SiPM technology. The detector calibration is presented, as well as preliminary results on the application of software compensation for the measurement of the energy resolution. The analysis of hadron shower development in the calorimeter using both data and Monte Carlo simulations is reviewed.

# 1 Introduction

The CALICE collaboration [1] is performing calorimeter development aiming to fulfill the hardware and physics demands of the International Linear Collider physics program [2]. The ambitious required jet energy precision ($30\%/\sqrt{E[GeV]}$) could be achieved with extremely segmented calorimeters using the particle flow approach [2].
The CALICE analogue hadron calorimeter prototype (AHCAL) is a 38 layer sampling calorimeter with 1 $m^2$ lateral dimension, and total thickness of 4.5 nuclear interaction lengths. Each layer consists of 2 cm thick steel absorber and a plane of 0.5 cm thick plastic scintillator tiles. The tile sizes vary from 3x3 $cm^2$ in the center of the layer, to 6x6 $cm^2$ and 12x12 $cm^2$ in the outer regions, providing in total 7608 readout channels for the entire calorimeter. Each tile is coupled to a silicon photomultiplier (SiPM) via a wavelength shifting fiber.
Together with the CALICE silicon-tungsten electromagnetic calorimeter (ECAL) and the CALICE tail-catcher and muon tracker (TCMT), the AHCAL was exposed to muon, electron/positron and hadron beams at the test beam line at CERN and FERMILAB in 2006-2007 and 2008, respectively. In 2008-2009 combined operations were additionally performed using a different technology for the electromagnetic calorimeter, the scintillator-tungsten ECAL. A typical test beam setup for the combined operations is presented in Fig. 1. The silicon-tungsten ECAL will be again used in test beam operations planned in 2010 along with a digital hadronic calorimeter and the TCMT. The results of the 2007 CERN data analysis are presented in this note.

# 2 Calorimeter calibration

The SiPM device (produced by MEPhI/Pulsar) is a multi-pixel (1156 pixels) avalanche photodiode which provides a signal gain factor of approximately $10^6$. The gain of each

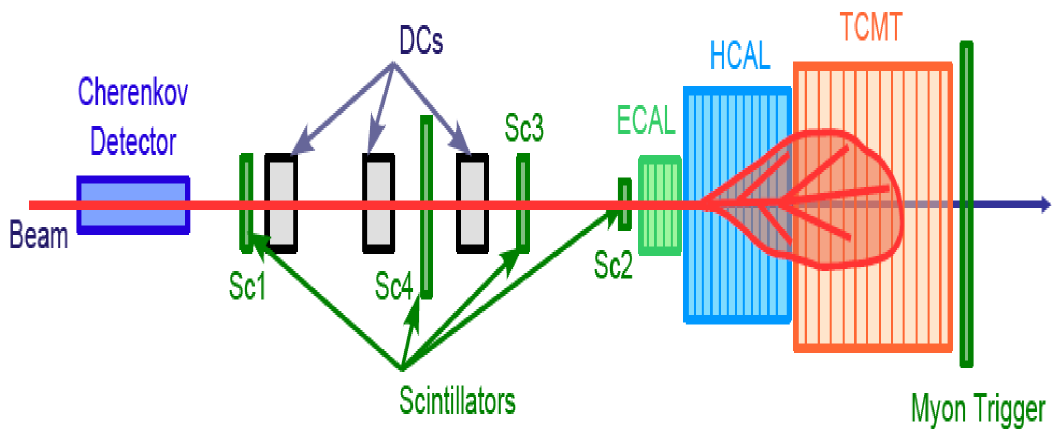


Figure 1: Typical test beam setup for the combined operations of the detectors ECAL, HCAL and TCMT.

SiPM is monitored via dedicated measurements during test beam data taking, illuminating the device with low intensity LED light [3]. During the extensive test beam operations at CERN a gain calibration for 97% of the channels was extracted, confirming the stable and high performance of SiPMs in a large scale calorimeter.
The energy deposited by a particle in the scintillating plate is read out by the SiPM, and converted into ADC units. The energy calibration was performed measuring the response to the passage of minimum ionising particles (mip), using muons as mips. The muon signal deposited in a tile was fitted with a Gaussian convoluted with a Landau distribution, and the most probable value of the distribution was assumed to be one MIP unit, corresponding to 0.861 MeV, as obtained with Monte Carlo simulations [4]. The systematic uncertainty on the energy calibration due to the intrinsic short-term operational variations of the detector properties was found to be approximately 3%. In the analysis, the rejection of hits with energy below 0.5 MIP results in a mip hit detection efficiency of about 95% [5].
Due to the limited number of pixels and to the finite pixel recovery time ($> 100$ ns), SiPMs are non linear devices. The reconstructed energy is corrected for non-linearity effects using response curves, measured individually for every SiPM [6]. SiPMs are temperature dependent devices. Therefore, a temperature monitoring system was implemented to measure and correct for the single pixel gain, and for the mip amplitude temperature dependence. The slope of the temperature dependence of the SiPM gain $G$ and of the SiPM response $A$ to a mip, averaged over all channels, was found to be $\frac{1}{G}\frac{d}{dT}G = -1.7\frac{\%}{K}$ and $\frac{1}{A}\frac{d}{dT}A = -3.7\frac{\%}{K}$ [7], respectively.

# 3 AHCAL response to positron showers

Being the description of underlying physics reasonably understood, Monte Carlo (MC) simulation of electromagnetic showers in the detector can be compared to the data to validate the calibration procedure, and to validate the detector effects introduced in the Monte Carlo simulation (digitisation).
After applying all the calibrations described above, the detector response to electromagnetic showers is measured at different beam energy values. The residuals to the linear fit to the data is shown in the upper panel of Fig. 2. Within both statistical and systematical uncertainties, the reconstructed response is linear up to 30 GeV beam energy. Superimposed to the data the MC prediction is also shown. The energy resolution is shown in the lower panel of Fig. 2, and compared with simulations with and without the inclusion of detector effects. The smearing effects included in the simulation improve the agreement, although the data still have systematically larger values than what is predicted by the simulations. This can be possibly understood considering that not all the calibration uncertainties have been included in the MC yet. Their inclusion should result in larger values of the simulated resolution.

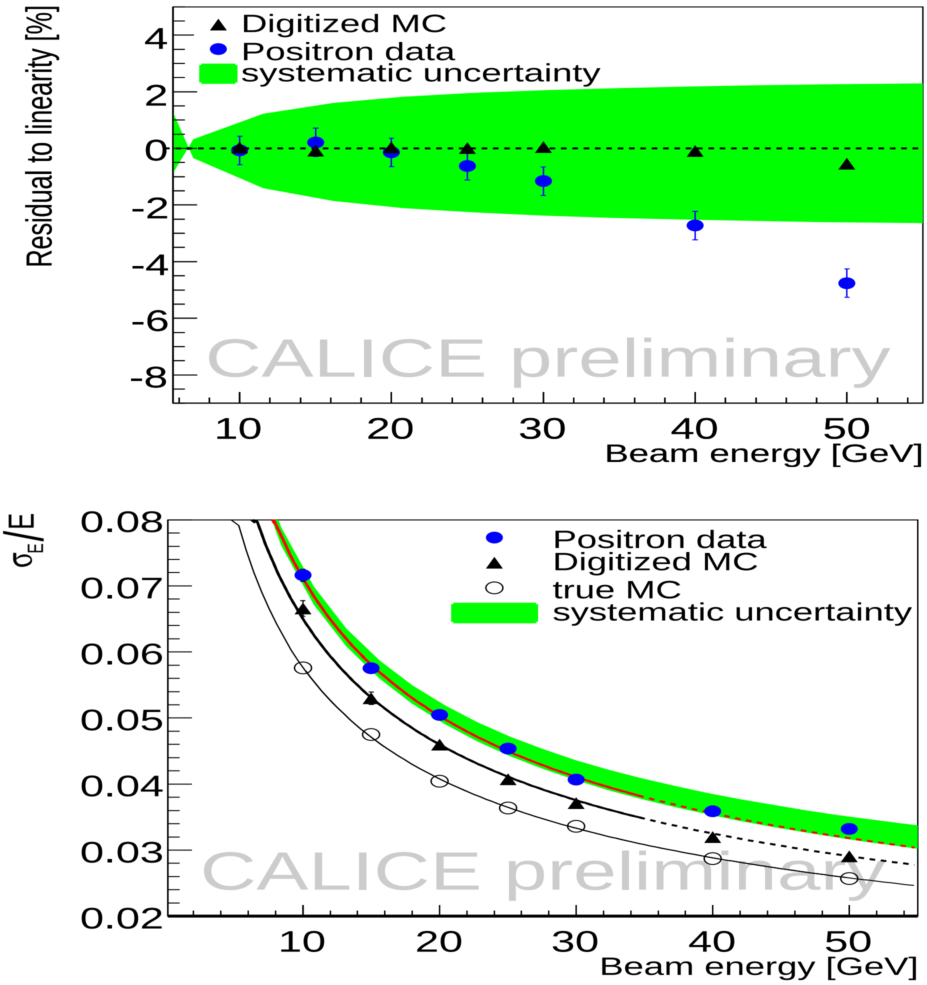


Figure 2: The residuals to the linear fit performed to the detector response to electromagnetic showers (upper panel), and the energy resolution to electromagnetic showers (bottom panel) are shown for both the data and MC. The largest contribution to the systematical uncertainty is given by the calibration uncertainties on both the MIP energy determination and the non-linearity effects correction.

## 4 Analysis of pion data

The understanding of electromagnetic showers in the AHCAL was shown to be reasonable for a preliminary analysis of hadronic showers. The high segmentation and granularity of the AHCAL calorimeter allows the investigation of the longitudinal and lateral shower profiles with unprecedent precision.
The fluctuations in hadronic shower development are larger than what is observed in electromagnetic showers. The high longitudinal segmentation of the AHCAL allows to

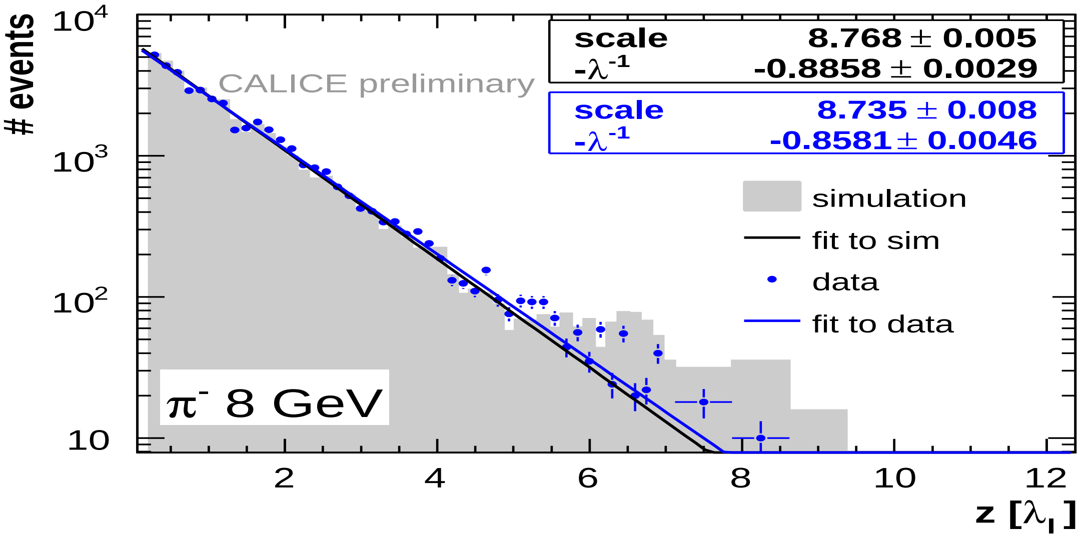


Figure 3: The exponential distribution of the first nuclear interaction in showers is measured versus the nuclear interaction length for 8 GeV $\pi^-$ mesons, and compared with MC simulations using the physics model list LHEP. The data shown here were collected in 2007, combining the information from both the AHCAL and TCMT devices rotated at $30^o$ with respect to the beam. The ECAL was removed from the beam line.

localise the shower starting point. An exponential fit to the distribution of the first interaction of showers as a function of the distance $z$ (in units of nuclear interaction length $\lambda_I$) from the start of the calorimeter was performed, and the interaction length for $\pi^-$ mesons was extracted [8], Fig. 3.
The effects of investigating the hadronic shower development with respect to the shower starting point are clearly evident in the analysis of longitudinal shower profiles, where the event by event fluctuation of the shower start position can be corrected for, Fig. 4 [9].

Knowing the energy of the impinging meson beam, the effects of longitudinal energy leakage in the shower development was measured for different values of the beam energy, Fig. 5 [9].

## 5 Investigation of hadron Showers

Different Monte Carlo physics model lists are available in the GEANT4 software package [10], and provide different predictions for the hadronic shower development, which can be constrained, in principle, by the precise results of the AHCAL. Hadron showers were investigated with unprecedented precision, and the agreement between data and Monte Carlo was found to be within 20%. Discrepancies were spotted depending on the model, impinging beam energy, and on the analysed observable.

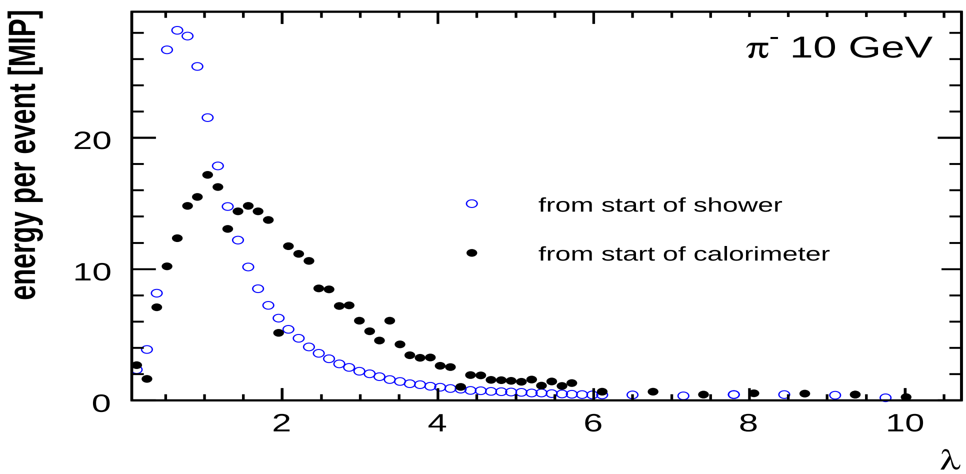


Figure 4: The longitudinal shower profile for a 10 GeV $\pi^-$ impinging meson beam is reconstructed in nuclear interaction length units with respect to the calorimeter and to the shower start location (filled and empty markers, respectively). The data shown here were collected in 2007, combining the information from both the AHCAL and TCMT devices rotated at $30^o$ with respect to the beam. The ECAL was removed from the beam line.

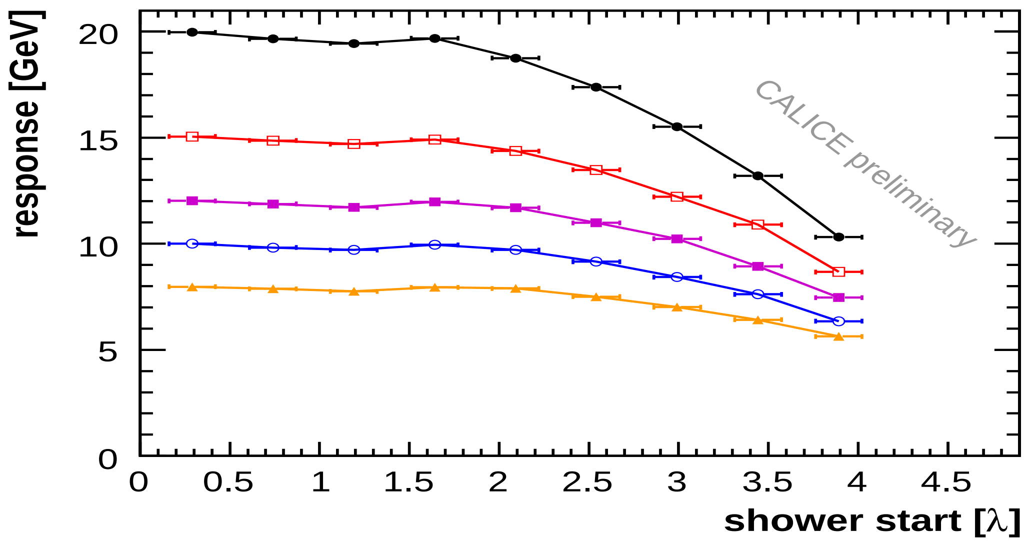


Figure 5: The shower longitudinal leakage is measured for different energy values of the impinging $\pi$ beam (8, 10, 12, 15, and 20 GeV, from top to bottom data sets). The data shown here were collected in 2007, combining the information from both the AHCAL and TCMT devices rotated at $30^o$ with respect to the beam. The ECAL was removed from the beam line.

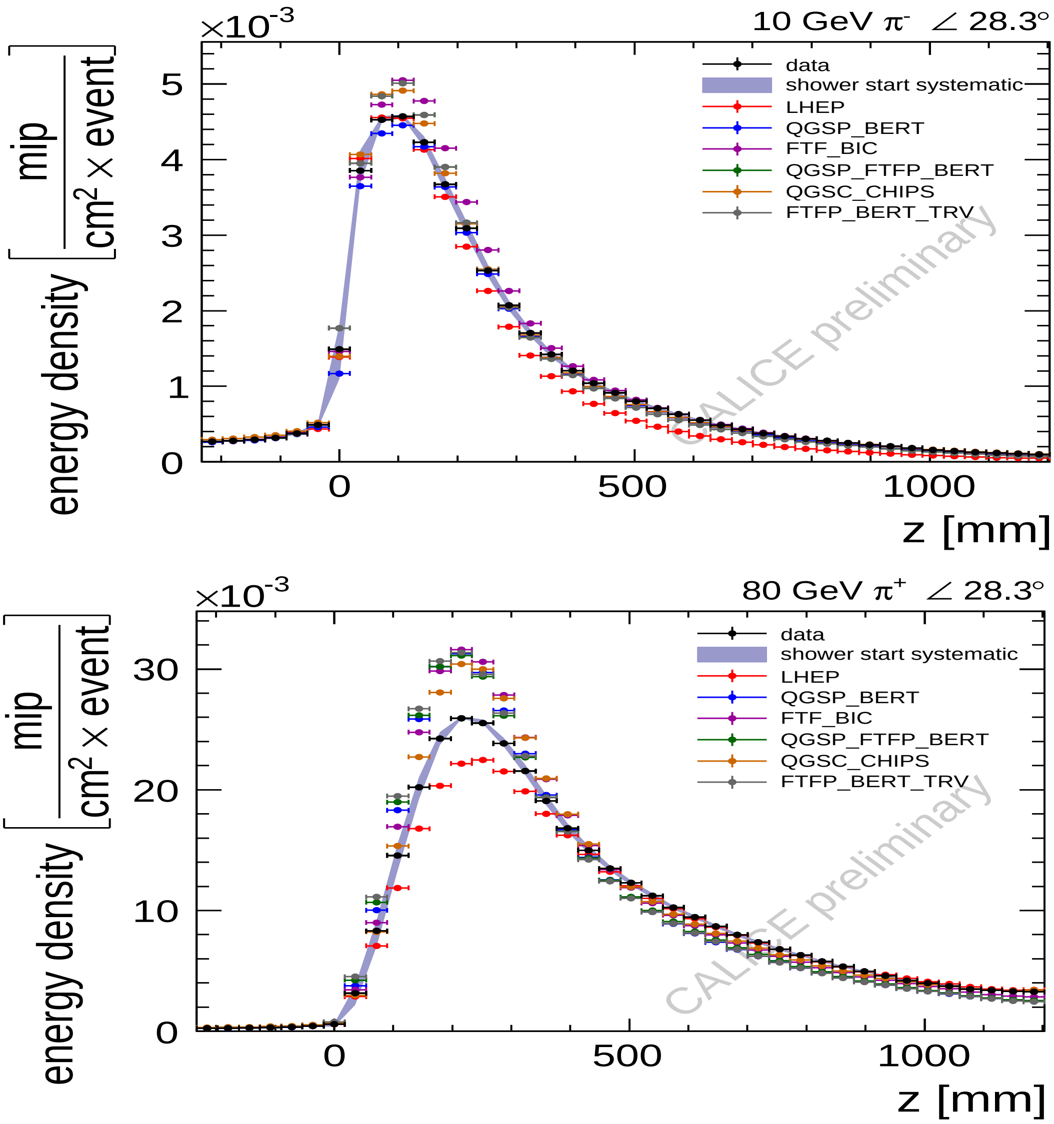


Figure 6: Longitudinal hadron shower profiles presented for 10 (upper panel) and 80 (lower panel) GeV $\pi$ meson beams. The data shown here were collected in 2007, combining the information from both the AHCAL and TCMT devices rotated at $30^o$ with respect to the beam. The ECAL was removed from the beam line. Superimposed to the data are shown GEANT4 based simulations.

The longitudinal profile (measured with respect to the shower starting point) is presented in Fig. 6 for 10 and 80 GeV $\pi$ meson beams [11]. Superimposed to the data are simulations performed using several physics model lists. Typically models predict higher density in the shower maximum and lower density in the tails.
The lateral shower profiles were also investigated, and the density of the deposited (visible) energy was measured in the AHCAL with respect to the primary track for

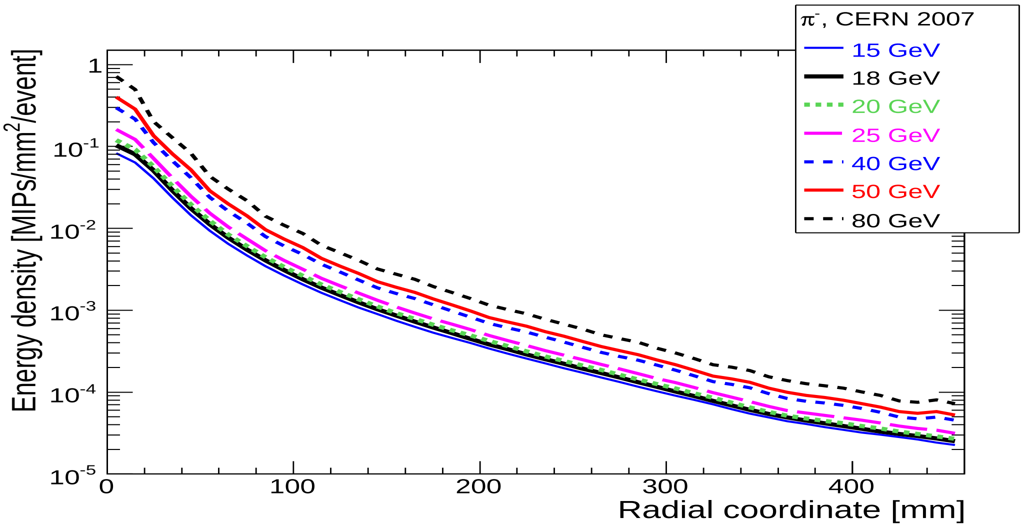


Figure 7: The lateral energy deposition is measured in the AHCAL for different values of the $\pi^-$ meson beam energy.

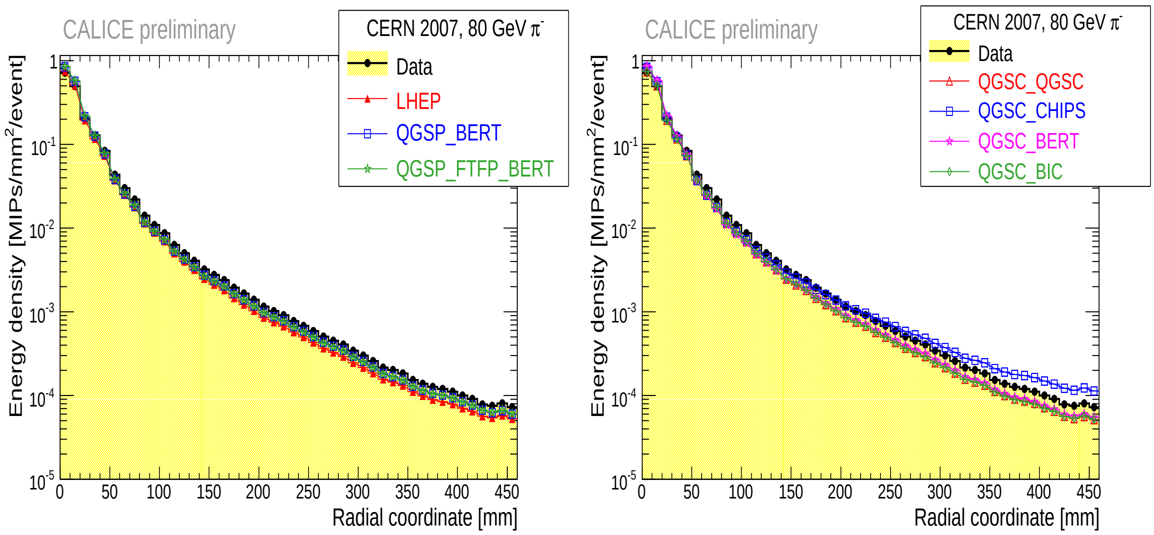


Figure 8: Simulations of the lateral energy deposition of hadron showers are compared in the AHCAL with the data for 80 GeV $\pi^-$ meson beam energy.

different test beam energies [12]. The results, presented in Fig. 7 for data only, show a weak dependency of the energy density on the beam energy.
Simulations are compared with the data in Fig. 8 for a 80 GeV $\pi^-$ meson beam, typically undershooting the data in the radial tail of profiles [12]. Typically models predict lower energy density in the shower lateral tails. Among the several investigated physics model lists, the QGSP_CHIPS list (which in average generates more neutrons than the other

lists) appears to provide the worst description of the data. However, the implementation of that model list in GEANT4 is still under development, and a definitive conclusion cannot be drawn at the moment.
For each event, the lateral shower radius can be measured by weighting the coordinates of the firing hits in one event with their corresponding visible energy. The mean of the distribution of the extracted values of the radius is presented in Fig. 9 for different energies of impinging $\pi^-$ mesons [12], for both data and Monte Carlo simulations. Predictions are typically lower than the data.
The high segmentation and granularity of the AHCAL allows the investigation of the longitudinal shower development in different bins of the radial profiles. Examples of this analysis [11] are presented in Fig. 10 and Fig. 11 for 10 and 80 GeV $\pi$ meson beams, and for the radial bins $0 < \rho \leq 6$ cm, $6 < \rho \leq 12$ cm, $12 < \rho \leq 18$ cm, and $18 < \rho \leq 24$ cm. Typically models predict higher energy density in the shower core, while a better agreement is observed at relative large radial distances (for low beam energy).

# 6 Conclusions

In this note the results of the successful CALICE data taking at CERN in 2007 were presented. The results verify the stable and high performance of SiPMs in a large scale calorimeter. The calibration procedure to establish the electromagnetic energy scale was described. The high segmentation and granularity of the calorimeter allowed the investigation of the longitudinal and lateral hadron shower profiles with unprecedent precision, thus providing possible constraints for Monte Carlo models. The analysis of the CALICE data is on going (also including the ECAL data, and the lower beam energy FERMILAB data) with the prospective to provide a detailed quantitative description of the hadron shower development.

# 7 Acknowledgement

This work is supported by the Commission of the European Communities under the 6th Framework Programme “Structuring the European Research Area”, contract number RII3-026126.

# References

[1] https://twiki.cern.ch/twiki/bin/view/CALICE/WebHome.

[2] J. Brau et al., International Linear Collider Reference Design Report, ILC-REPORT-2007-001 (2007).

[3] N. Wattimena, DESY-THESIS-2006-039.

[4] N. D’Ascenzo, DESY-THESIS-2009-004.

[5] F. Sefkow, Proc. of The International Workshop on new Photon-Detectors (Kobe, Japan, 2007), PoS(PD07)003.

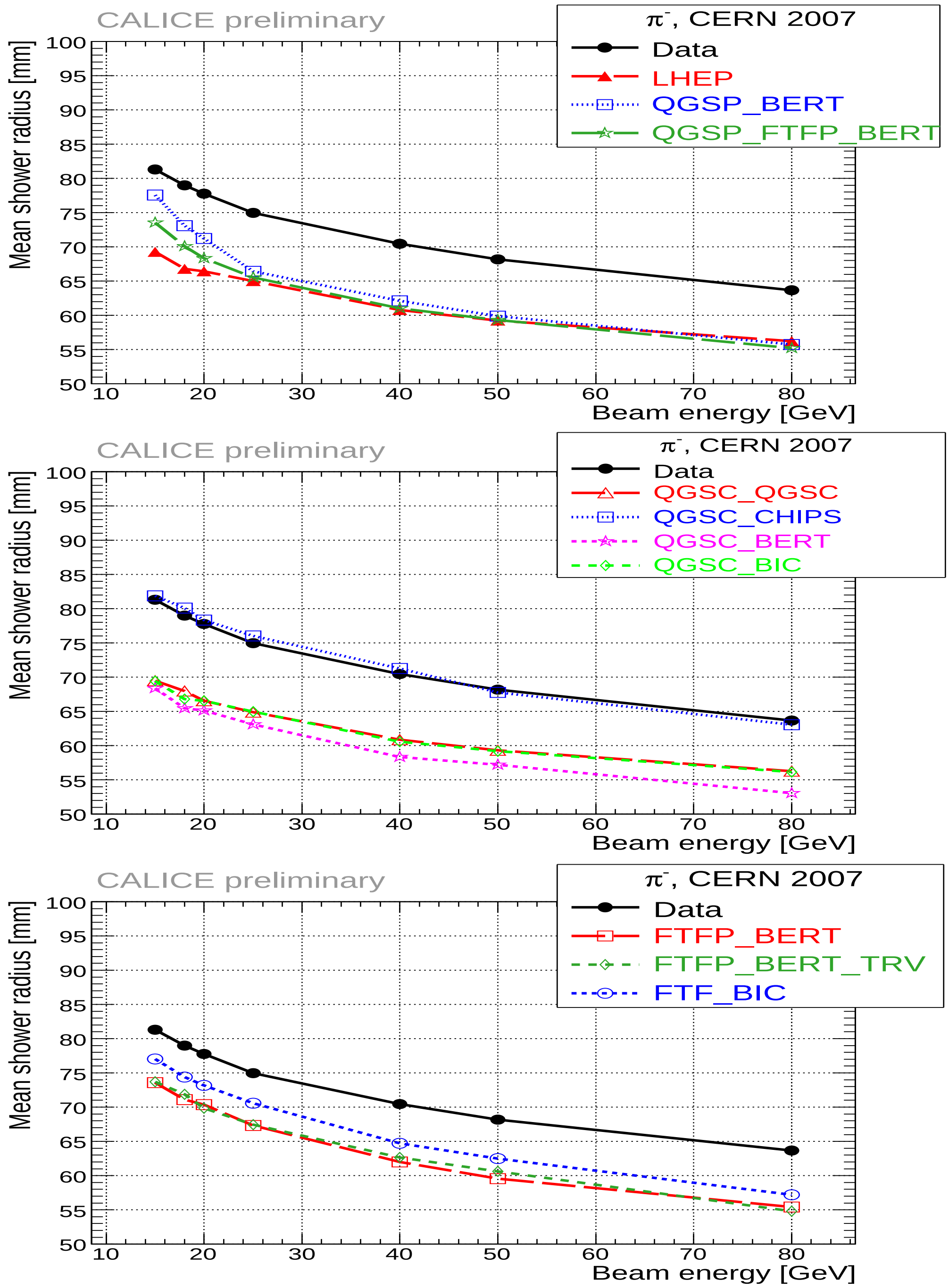


Figure 9: The mean shower radius, calculated as described in the text, is presented for different energies of the $\pi^-$ meson beam, and is compared with GEANT4 based simulations. The data shown here were collected in 2007, using only the information from AHCAL.

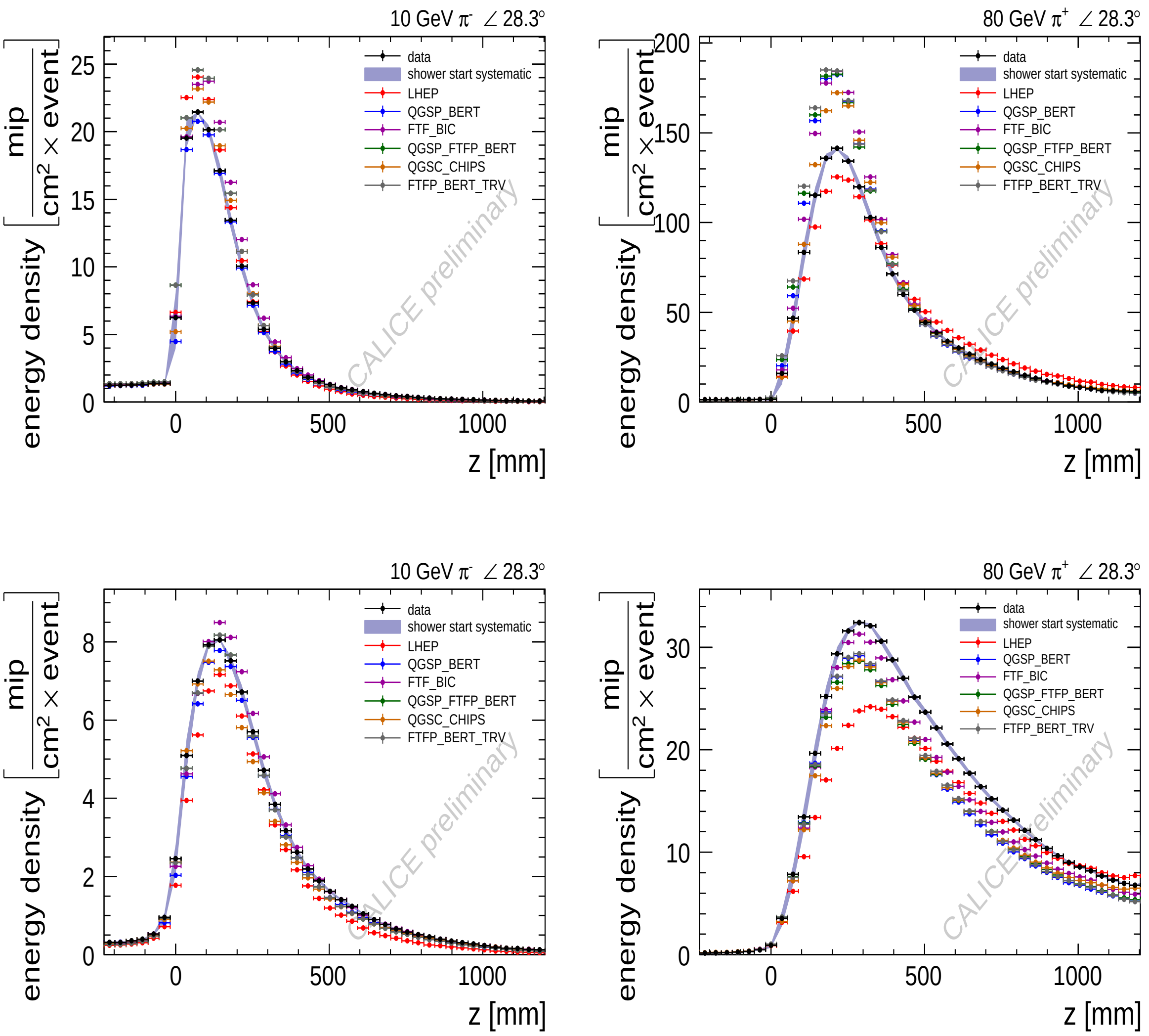


Figure 10: The longitudinal hadron shower profile is presented for the 10 GeV $\pi^-$ (left panels) and the 80 GeV $\pi^+$ (right panels) meson beam in the radial bins $0 < \rho < 6$ cm and $6 < \rho < 12$ cm (upper and lower panel, respectively). The data shown here were collected in 2007, combining the information from both the AHCAL and TCMT devices rotated at $30^o$ with respect to the beam. The ECAL was removed from the beam line. Superimposed to the data are shown GEANT4 based simulations.


[6] N. Wattimena (for the CALICE Collaboration), Proc. of International School of Subnuclear Physics ISSP07 (Erice, Italy, 2007).

[7] N. Feege, DESY-THESIS-2008-050.

[8] CALICE Collaboration, CAN-011 (2007).

[9] B. Lutz (for the CALICE Collaboration), Proc. of the 2008 IEEE Nuclear Science Symposium (Dresden, Germany, 2008).

[10] J. Apostolakis et al., CERN-LCGAPP-2007-02.

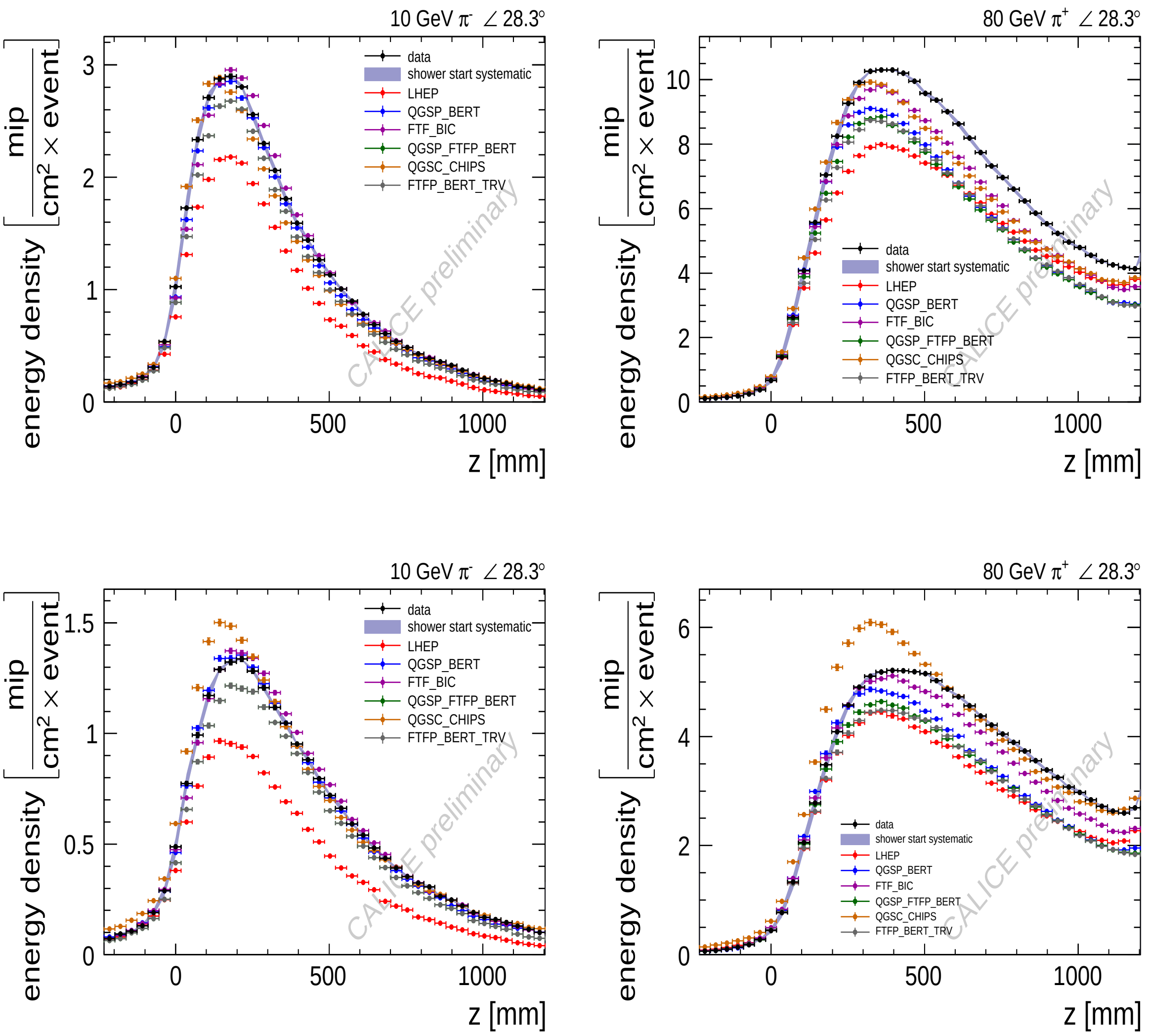


Figure 11: The longitudinal hadron shower profile is presented for the 10 GeV $\pi^-$ (left panels) and the 80 GeV $\pi^+$ (right panels) meson beam in the radial bins $12 < \rho < 18$ cm and $18 < \rho < 24$ cm (upper and lower panel, respectively). The data shown here were collected in 2007, combining the information from both the AHCAL and TCMT devices rotated at $30^o$ with respect to the beam. The ECAL was removed from the beam line. Superimposed to the data are shown GEANT4 based simulations.

[11] CALICE Collaboration, CAN-011d (2009).

[12] CALICE Collaboration, CAN-011e (2009).